A theoretical study of the XANES spectra of rutile and anatase

1991 J. Phys.: Condens. Matter 3 8981

(http://iopscience.iop.org/0953-8984/3/45/019)

J. Phys.: Condens. Matter 3 (1991) 8981–8990. Printed in the UK

A theoretical study of the XANES spectra of rutile and anatase

M F Ruiz-López† and A Muñoz-Páez‡

† Laboratoire de Chimie Théorique, Université de Nancy I, BP 239, 54506 Vandoeuvre les Nancy, France

‡ Departamento de Química Inorgánica, Universidad de Sevilla, Apdo. 553, 41071 Sevilla, Spain

Received 4 June 1991, in final form 6 August 1991

Abstract. A model based on the local density approximation and on the multiple-scattering wave method has been used to analyse the experimental XANES spectra of the crystalline materials rutile and anatase. The results presented in this work are close to the best computations that can be achieved for the solid adopting a local density one-electron theory. The effect of cluster size on the computations has been analysed in the case of rutile concluding that at least 51 atoms are needed to get all the spectral features. Convergence is obtained for a model comprising 75 atoms. The agreement between the theoretical and the experimental spectra is very good even for the pre-edge structures, the origin of which has been the object of controversy. Minor differences, which could be assigned to many-body effects, have been pointed out. SCF Xα computations have also been performed and allow the formulation of some hypotheses concerning two-electron excitations in the XANES spectra.

1. Introduction

Titania catalyses several photo-assisted processes, like partial oxidation of hydrocarbons, decomposition of water (to form H_2 and O_2) and reduction of N_2 to NH_3, due to its semiconducting oxide character [1]. The acid-base properties of its surface make it active in alcohol decomposition. In addition it has been widely used as support in metal catalysts due to its surface and bulk properties and to its ability to increase the activity and selectivity of the metal in hydrogenation/dehydrogenation processes [2].

When acting as a catalyst or support, this oxide is in most cases in the crystalline forms of anatase (stable at low temperature) or rutile (stable above 700 °C). Nevertheless, there is an increasing interest in amorphous TiO_2 based systems in the field of catalysis, due to the high efficiencies of the 'mixed' or 'surface' oxides (where titanium oxide is deposited or embedded in a matrix of a second oxide to increase the surface area and thus catalytic selectivity and/or activity), and in the field of materials science to prepare titania glasses and ceramics [3].

Since these systems do not show long-range order around Ti atoms, x-ray absorption spectroscopy (XAS) is a unique tool to get information on their structure. Thus, the spectra of several titanium compounds, crystalline and amorphous oxides, alcoholates, chlorides, have been measured, and the XANES region of these spectra have been the subject of several theoretical and experimental studies [4–16]. Nevertheless, this region is far from being understood. For instance, Emili *et al* [5] have related the pre-edge of Ti with the coordination geometry around Ti centres, in TiO_2–SiO_2

0953-8984/91/458981+10$03.50

glasses, while Asbrink *et al* [7] have related the same feature to oxidation state in TiO_2–VO_x systems. On the other hand, Grunes [4] has assigned the features of the anatase and rutile edges on the basis of calculations for TiO_6 octahedra, but these units do not reproduce the periodicity and the long-range order present in the crystalline structures. The work by Brydson *et al* [10] is more complete, where the XANES spectrum for a system with several atomic shells has been computed using a multiple-scattering formalism.

All these studies reveal the importance of titanium oxides and titanium based systems, as well as the difficulties in understanding the XANES region of the x-ray absorption spectra, nearly the only tool to obtain information about coordination geometries in the amorphous systems. The first step towards understanding these spectra is, in our opinion, the thorough study of the spectra of the crystalline oxides, having a well known structure.

The use of one-electron theories and in particular those derived from the local spin density approximation, such as the $X\alpha$ method, has been useful to interpret many experimental results in x-ray spectroscopy. In this paper we present detailed theoretical computations for the crystalline titanium oxides rutile and anatase.

2. Experimental section

XAS experiments were performed on the EXAFS station 8.1 in the synchrotron radiation source at Daresbury Laboratories with ring energies of 2 GeV and ring currents of 250 mA. The EXAFS spectrum was recorded at −198 °C in an *in situ* cell, where the sample was placed after being pressed with BN into a wafer with an absorbance (μx) of 2.5 at the titanium K-edge, assuring an optimum signal/noise ratio.

3. Computations

The edge spectra have been computed using a multiple-scattering program described elsewhere [17]. As a first step one has to define a local density potential for the system. If a convenient approximation for this potential has been determined, the initial state (a bound core level) and the final state (an electron in the continuum) may be computed and the total cross section is given by

$$\sigma = 4\pi^2 \alpha \hbar\omega \sum_{\mathrm{f}} |\langle \phi_{\mathrm{f}} | \epsilon \cdot r | \phi_{\mathrm{i}} \rangle|^2 \qquad (1)$$

where $\alpha = e^2/\hbar c$, $\omega = E - E_o$ and $\epsilon \cdot r$ is a component of the transition moment operator between the initial state ϕ_{i}, usually 1s, 2s, 2p, ..., and a final electronic state in the continuum ϕ_{f}. Following most of the reported computations in this field, we use a muffin-tin type potential. Moreover, due to the large number of atoms considered, the potential is estimated by an average sum of atomic potentials. Obviously this is a crude approximation but previous work has shown that it gives reasonably good results, especially in the case of very symmetric systems such as those studied here. A non-muffin-tin version of the MS program has been recently developed [18] but for large systems its use is still too expensive. The muffin-tin radii used in this work were obtained according to the Norman criterion and so that the atomic spheres are almost tangent: this gives $R_{\mathrm{Ti}} = 2.04$ au and $R_{\mathrm{O}} = 1.66$ au.

Theoretical spectra are also quite sensitive to the type of the local density approximation for the exchange-correlation potential. In this work we use the energy-dependent Dirac–Hara exchange potential [19] which seems to give the best results in XAS studies [20,21]. The spectra are then convoluted to account for inelastic losses using the Hedin–Lundqvist [22] approach which permits calculation of the effective mean free path of the photoelectron at a given kinetic energy. This requires computation of the local momentum functional:

$$p^2(\boldsymbol{r}) = k^2 + k_F^2(\boldsymbol{r}) \tag{2}$$

where k^2 is the photoelectron kinetic energy measured from the Fermi level and $k_F = [3\pi^2\rho(\boldsymbol{r})]^{1/3}$ is the local Fermi energy. The Fermi level has been estimated in this work as an intermediate value between the interstitial potential and the potential at infinity as obtained using the Xα functional and an outer sphere. In the case of rutile, the Fermi level is -0.29 Ryd and the interstitial charge density is equal to 1.28×10^{-2} au. Similar values have been obtained for anatase. The core-hole lifetime, which may be related to an effective mean-free path, has been ignored in our computations. It should be pointed out that the theoretical spectra are computed in an energy scale relative to the muffin-tin constant potential; then, the spectra are shifted in order to be compared with experimental data.

4. Results and discussion

4.1. Description of the models

In rutile and anatase, octahedral groups of oxygen atoms are placed around a titanium atom and every oxygen atom is between three titanium atoms. They are both tetragonal and the main structural differences lie in the way the octahedra are deformed and linked together. For a description of their crystal structures see for instance [23]. In our computations we shall consider clusters of atoms consisting of one Ti atom surrounded by a given number of neighbouring atoms for which the distance with respect to the central Ti atom (the absorbing atom) is shorter than a given value. The basic unit is a deformed octahedron with two different Ti–O distances. In rutile there are four Ti–O distances at 1.946 Å and two at 1.984 Å . The symmetry group is D_{2h}. In anatase, the corresponding distances are 1.937 Å and 1.964 Å and the symmetry group is D_{2d}.

The computation of the XANES spectrum of a crystalline solid requires the choice of a convenient model representing the electronic properties of the solid as well as possible. Owing to computational limitations the number of atoms considered should not be very large but keeping this number too small could lead to inaccurate or even unrealistic results. So we have regarded detailed analysis of the effect of cluster size on computations as crucial. Results will be presented in the case of rutile.

4.2. Rutile spectrum

Figure 1 compares the results obtained for the K-edge spectrum of several models of rutile with increasing number of atomic shells. All these computations have been performed using the simple Xα potential. The models are summarized in table 1. An additional computation for a model including a total number of 105 atoms did not

change the results of the 75 atoms model appreciably and is not included in the figure. From these results one concludes that at least 51 atoms (model 3) should be included in the computations in order to get all the spectral features, whose intensity, however, may still be modified by further shells. A good convergence is obtained for model 4 (75 atoms). This model includes all atoms lying in a radius of 5.5 Å so that one can consider that scattering paths of total length greater than about 11 Å contribute little to the absorption. In other words, this model allows a good description of the electronic properties of the solid.

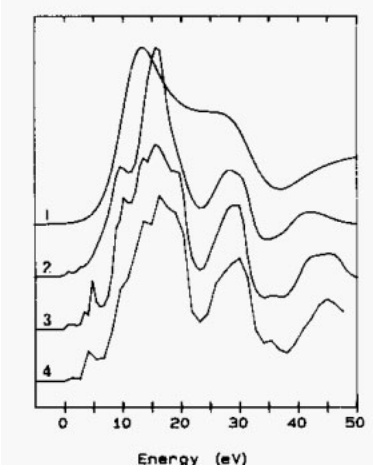

Figure 1. Computed XANES spectra (arbitrary scale) for model systems of rutile with different dimension: 1) Model 1 (TiO_6), 2) Model 2 ($Ti_{11}O_{14}$), 3) Model 3 ($Ti_{15}O_{36}$) and 4) Model 4 ($Ti_{31}O_{44}$).

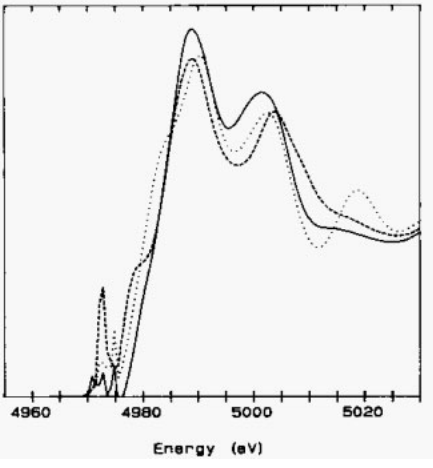

Figure 2. Components of the rutile (model 4) spectrum (arbitrary scale) computed with the Dirac–Hara potential for the polarizations $x(b_{3u})$ (dash), $y(b_{2u})$ (dot), $z(b_{1u})$ (single).

Table 1. Models for crystalline TiO_2 rutile.

Model	No of atoms		No of shells[a]	Radius (Å)[b]
	Ti	O		
1	1	6	1	1.983
2	11	14	3	3.569
3	15	36	5	4.615
4	31	44	6	5.500
5	37	68	9	6.495

[a] Shells are separated by at least 0.2 Å.
[b] Distance of the absorbing Ti atom to the most distant atom.

It is interesting to point out that pre-edge features are observed for models 2, 3 and 4 and that their intensity is quite sensitive to the number of atoms considered. We shall discuss this point later.

The results obtained in the case of model 4 for the three possible absorption polarizations (which according to group theory are associated with the b_{1u}, b_{2u} and b_{3u} irreducible representations) are presented in figure 2. We now use the more elaborate

Dirac–Hara exchange potential. Pre-edge features are predicted for all polarizations, the b_{3u} giving the most substantial contribution. Below the edge, the three curves exhibit quite similar shapes except that a resonance is observed at 40 eV beyond the edge for b_{2u} polarization. The maxima of the curves are of course associated with electronic transitions to the diffuse np orbitals, with increasing n. The sum of these curves is compared to experimental data in figure 3. Most of the experimental peaks are correctly predicted by the computations: the relative intensities for the three pre-edge features A_1, A_2, A_3, the edge feature B and the resonances D and E are computed reasonably well. For features C_1 and C_2 the agreement is not so good but our results require some comments. In the computed spectrum of figure 3, only one peak (c) seems to be present while in the experimental spectrum two peaks (C_1 and C_2) are clearly observable. A detailed analysis of the computations shows a shoulder in the computed spectrum between b and c corresponding to a shoulder in the b_{2u} symmetry component (see figure 2). In the Xα computation (see figure 1), this gives a flat maximum in the spectrum that the Hedin–Lundqvist convolution tends to erase. Thus, the theoretical model predicts two features in this region, in agreement with experiment, but the computations fail to reproduce the energy separation and the relative intensities correctly. Reasonable modifications of the sphere radii do not change these results much, only the absorption intensity in the pre-edge region being quite sensitive to the muffin-tin model parameters. Apart from the usual limitations inherent to the use of a muffin-tin model potential, the main approximation made in our calculations is the use of a one-electron theory which does not take into account many-body interactions. In fact, the presence of shake-down transitions has been previously proposed [6] to explain the origin of peak C_1. The use of a more complete many-body theory, such as the configuration interaction approach or the random phase approximation, would be necessary to evaluate the transition intensities and to obtain a definitive conclusion, but this type of calculation is still prohibitive for complex systems. However, we shall discuss below the nature of the possible multi-electron excitations involved.

4.3. Anatase spectrum

The computed spectrum for anatase is compared to experimental data in figure 4. The model used for anatase is comparable to that used for rutile, i.e., all atoms within a sphere of radius 5.5 Å around the absorbing Ti atom are included; this gives a cluster of 63 atoms ($Ti_{29}O_{34}$).

The spectra of anatase and rutile present substantial differences which reflect their different long-range order. Most of the remarks made for rutile also stand for anatase. Notice that, again, a single peak (c) is predicted. Feature (d) is computed at a lower energy than the corresponding peak in rutile, in agreement with experimental data although the experimental spectrum has more than a single structure. The resonance labelled E in rutile is not present in anatase but a weak signal is observed at about 5017 eV in the experimental spectrum of anatase.

4.4. Pre-edge structures

In centro-symmetric systems like rutile, the 1s → 3d transitions are dipole-forbidden by symmetry conditions (s and d orbitals have g symmetry, i.e. they do not change sign under inversion, while the dipole moment operator has u symmetry and changes sign). One may however expect this transition to become 'allowed' by higher-order

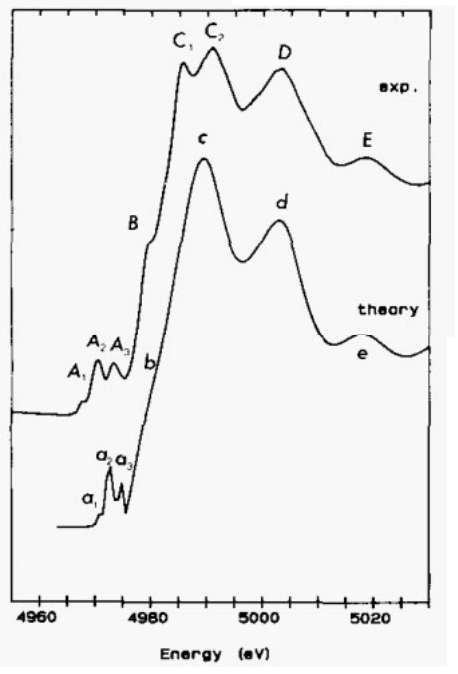

Figure 3. Comparison between the experimental spectra of rutile (top) and the computed spectra using model 4 and the Dirac–Hara potential (bottom). The spectra are plotted in an arbitrary scale but the theoretical curve has been normalized so that the intensity of peak C is equal to that of the experimental curve.

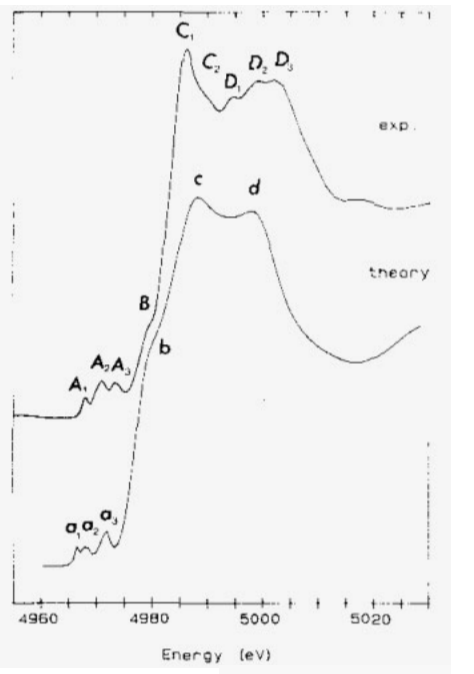

Figure 4. Comparison between the experimental spectra of anatase (top) and the computed spectra using a model equivalent to model 4 in rutile (bottom). The Dirac–Hara potential is used. The spectra are plotted in an arbitrary scale but the theoretical curve has been normalized so that the intensity of peak C is equal to that of the experimental curve.

multipole mechanisms or via vibronic coupling. Recent measurements of angle resolved edge spectra [14, 15] have shown that this part of the TiO_2 spectrum is sensitive to the orientation in a way consistent with a quadrupole mechanism. Temperature dependence of these peaks has also been pointed out [24] suggesting a possible vibronic coupling. Of course none of these mechanisms can be disregarded in principle although their intensity is probably small anyway.

In anatase (which has D_{2d} symmetry), 1s $\rightarrow$ 3d transitions are symmetry allowed but in spite of that, their intensity is slightly weaker than in rutile. This seems to indicate that the final states are not only described by the orbitals of the absorbing Ti atom, but that solid effects, i.e., mixing with the p and d bands, also have to be taken into account. In fact, our computations, which are limited to the dipole transition moment operator, show that the intensity of the transitions depend substantially on the number of atoms included in the computation, suggesting that the pre-edge structures are dipole allowed transitions to highly delocalized virtual orbitals in which the main contribution arises from Ti atoms. In order to evaluate the role of quadrupolar transitions we have calculated the corresponding intensity for the electron excitations 1s $\rightarrow$ 3d in a small model cluster TiO_6. The largest value is obtained for transitions to the $d_{x^2-y^2}$, d_{xz} and d_{yz}, i.e. the lowest energy crystal field orbitals. However, it

represents a negligible contribution to the total intensity (about 0.5% of the dipolar intensity computed for model 4).

Pre-edge structures with dipolar origin were also obtained in a similar computation by Brydson *et al* and were interpreted through 3d–4p orbital mixing which introduces some p character in the d bands. Indeed, symmetry considerations show that the p orbitals of the central Ti atom can mix with the d orbitals of the neighbouring Ti atoms. In centrosymmetric systems some u combinations between d orbitals are then possible. Their position will be modified following the ligand field and the interactions with the oxygen p orbitals but their energy will be not far from that of the d orbitals of the central Ti atom. Figure 5 shows this p–d mixing schematically in the case of rutile. Note that the d orbitals of neighbouring Ti atoms may belong to any of the irreducible representations of the symmetry group and as a consequence give rise to combinations which may be antisymmetric, namely b_{1u}, b_{2u} and b_{3u}. The intensity of the transitions to these orbitals is proportional to the weight of the central Ti p orbital in the combination. On the other hand, the p character depends on the Ti–Ti distance and will decrease for increasing values of this distance. This may explain why the intensity of these transitions is slightly greater in rutile (for which the distance of the central Ti to the closest Ti shells are 2.96 Å and 3.57 Å) than in anatase (where the corresponding values are 3.04 Å and 3.78 Å).

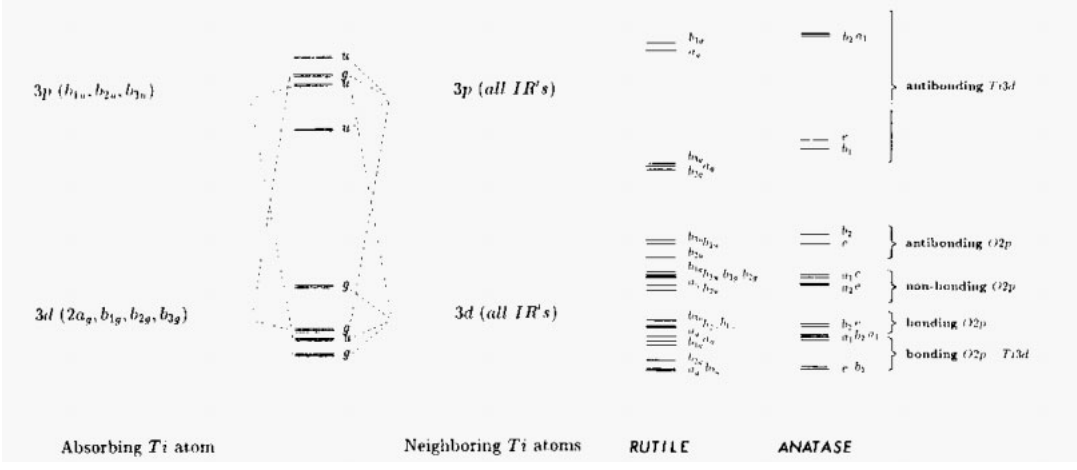

Figure 5. Orbital scheme for Ti–Ti orbital mixing.

Figure 6. Orbital scheme for the excited state $(1s)^1(4p)^1$ of rutile and anatase as computed with the Xα-MS-SCF method.

4.5. Orbital diagrams for TiO_6^{8-} and multi-electron effects

The theoretical computation of absorption intensities associated with multi-electron excitations is a difficult problem which would require configuration interaction computations for a system large enough to model the solid state properties. This type of calculation is at present beyond the usual computer capabilities and one can only obtain some qualitative results based on very approximate calculations. We present here a qualitative discussion of possible multi-electron effects on the basis of the

comparison of the orbital diagrams for the simplest model of rutile and anatase TiO_6^{8-}.

Previous SCF-MS computations have been reported for octahedral units of TiO_6^{8-} [25–27] and show that the Xα method is able to reproduce many spectroscopic properties of TiO_2 minerals. In this work, we have made SCF computations for the electronic ground state of TiO_6^{8-} with the geometrical parameters of rutile or anatase. We follow the procedure detailed by Tossell *et al* [25] except that the Madelung potential (used only to shift the energy levels) is replaced by the potential computed for a Watson sphere of charge +8 and the same radius as the outer sphere. Then an SCF computation is performed for an excited state with one hole in the Ti 1s orbital and one electron in the diffuse Ti 4p orbital. This state may be considered as a reference for the main absorption structure so that transition state computations may be performed to obtain relative energies for the two-electron transitions. The orbital diagram for such a state is plotted in figure 6 for the occupied valence orbitals (except for O 2s orbitals) and for the lowest unoccupied orbitals.

The occupied orbitals (all orbitals with negative energy $\epsilon_{X\alpha}$) may be divided into several groups. The first group of occupied orbitals lie between 2.5 and 3.5 eV and contain the Ti–O bonding orbitals which are linear combinations of metal 3d and oxygen 2p orbitals. Slightly below 2 eV, one finds a group of orbitals (b_{1u}, b_{2u}, b_{3u}, for rutile; b_2, e, for anatase) containing a total of six electrons (one per O^{2-} anion) which are combinations of oxygen 2p orbitals and have some bonding character. We shall refer to them as the 'bonding' O 2p orbitals. Their 'antibonding' partners are the highest occupied molecular orbitals which have slightly negative energies. The other orbitals in the energy region between −2 and 0 eV are non-bonding O 2p orbitals and contain the electron pairs. The molecular orbitals with positive energies are the metal 3d orbitals. They correspond to the octahedral t_{2g}, e_g, 'crystal field' orbitals. Because of the shorter Ti–O distances in anatase, these orbitals are slightly more destabilized in this case.

As we have pointed out, the multiple structures observed in peaks C and D of the spectra, are probably related to two-electron transitions consisting in a simultaneous excitation of a core electron, namely 1s → np, and of a valence electron. This last excitation must be a *monopole* transition, i.e., the symmetry of the initial and final orbitals must be the same. If one further assumes that the final orbital implied in the *monopole* transition is a metal 3d orbital (the energies of the other virtual orbitals are too high), then the following transitions can be considered: (i) d → d* transitions, where the excited electron is initially in one of the bonding O 2p–Ti 3d orbitals, (ii) transitions from the non-bonding O 2p orbitals, and (iii) transitions from the 'bonding' and 'antibonding' O 2p orbitals, which are only possible in the case of anatase, by symmetry conditions, and could be at the origin of the D structures observed in anatase. Transition state computations have shown that these excitations do not give shake-down effects, i.e., the energy of the two-electron excitation is always higher than the reference single excitation 1s → 4p. On the other hand, transitions arising from the non-bonding O 2p orbitals to the first set of virtual 3d orbitals (the octahedral t_{2g} orbitals) are the only processes for which the excitation energy is close to the C_1–C_2 energy separation in both rutile and anatase. Thus, in rutile, transitions O 2p(b_{2g}) → Ti 3d(b_{2g}) and O 2p(b_{3g}) → Ti 3d(b_{3g}) lie at 3.4 and 3.6 eV over the main 1s → 4p transition whereas in anatase there are two excitations O 2p(e) → Ti 3d(e) at 3.0 and 3.8 eV. It is interesting to point out that in tetrahedral $3d^0$ compounds including VO_4^{3-}, CrO_4^{2-} and MnO_4^-, two-electron excitations have been

identified both at low energy and at 40–50 eV above the edge [28]. A charge transfer transition O 2p → Ti 3d is at the origin of the low energy excitation (5 eV above the white line). The other excitation has been associated with a simultaneous 1s → 3d and 3p → 3d excitation; the corresponding excitation in TiO_6^{8-} is predicted at 42 eV. This value compares well with the energy of the feature at 5017 eV relative to the edge in anatase. In rutile, again, this type of transition is symmetry forbidden.

5. Conclusion

The results presented in this work illustrate the difficulties in computing XANES spectra for crystalline compounds. Computations have been carried out using a model based on the local density approximation and on the multiple-scattering wave method. This model may be successfully used only if a large number of atoms is included in the computation because the scattering amplitudes are extremely sensitive to long-range solid effects. Previous XANES calculations of complex systems [20,21,29,30] have also emphasized the effect of the cluster size on the results. In addition, the shape of the spectrum may be substantially perturbed by multi-electron effects rendering very complex the analysis of experimental data for these systems.

In rutile and anatase, the model allows prediction of most of the spectral characteristics and, in particular, the pre-edge structures which have been the subject of some controversy. Our computations show that these features may be easily explained by a mixing of 4p orbitals of the absorbing atom and 3d orbitals of neighbouring Ti atoms. The degree of orbital mixing and then the pre-edge intensity, is related, at least in part, to the Ti–Ti distances.

Our computations may be compared with the results of a previous theoretical study of the form peaks of the spectra [10]. For instance, in [10] pre-edge features have also been obtained as dipolar transitions and in the case of rutile only one peak, C, is predicted by the calculations. Nevertheless, our results are in better agreement with experiment, which is due to the use of a larger cluster size and an energy dependent exchange-correlation potential.

The main difference between the computed and the experimental spectra lies in the multiple structures observed in the vicinity of the 1s → np transitions that the theory fails to predict. These structures could be associated with multi-electron transitions. Some qualitative considerations based on SCF computations for TiO_6^{8-} indicate that all these transitions include charge transfer excitations from O 2p orbitals to virtual metal 3d orbitals. Only some selected orbitals (those containing the O electron pairs) may be invoked to explain the splitting of peak C in the spectra. More work is still necessary to reach a definitive conclusion about the role played by many-body effects in XANES. Better knowledge of these effects will not only increase the precision of the structural data obtained but also will give valuable informations on the electronic structure and correlation in these systems.

Acknowledgments

We thank C R Natoli for helpful discussions and for allowing us to use his programs for XANES and quadrupole transition computations. We also thank the Spanish DGICYT (project number PB 89-642) for financial support and the staff in the SRS

(Daresbury Laboratory, SERC, UK) for help during the XAS measurements. Finally, thanks are due to P E Hoggan for correcting the English.

References

[1] Kung H *Studies in Surface Science and Catalysis* vol 45; *Transition Metal Oxides* ed B Delmon, J T Yates 1989 (Amsterdam: Elsevier) ch 10 and 14
[2] Foger K 1984 *Catalysis, Science and Technol.* **6** 227
[3] Gesser H D and Goswami P C 1989 *Chem. Rev.* **89** 765
[4] Grunes L A 1983 *Phys. Rev.* B **27** 2111
[5] Emili M, Incoccia L, Mobilio S, Fagherazzi G and Guglielmi M 1985 *J. Non-Cryst. Solids* **74** 129
[6] Poumellec B, Marucco J F and Touzelin B 1986 *Phys. Status Solidi* b **137** 519
[7] Asbrink S, Greaves G N, Hatton P H and Garg K 1986 *J. Appl. Cryst.* **19** 331
[8] Babonneau F, Docuff S, Leaustic A, Sanchez C, Cartier C and Verdaguer M 1988 *Inorg. Chem.* **27** 3166
[9] Kuetgens U and Hormes J 1990 *2nd European Conf. Prog. x-ray Synch. Rad. Res.* 1990 vol 25, ed A Balerna, E Bernieri, and S Mobilio (Bologna: SIF) pp 59–62
[10] Brydson R, Sauer H, Engel W, Thomas J M, Zeitler E, Kosugi N and Kuroda H 1989 *J. Phys.: Condens. Matter* **1** 797
[11] Muñoz-Páez A and Munuera G 1991 Preparation of catalyst V *Studies in Surface Science and Catalysis* vol 62, ed G Poncelet, P A Jacobs, P Grange and B Delmon (Amsterdam: Elsevier) p 627
[12] Van der Laan G, Mythen C S and Padmore H A 1990 *Europhys. Lett.* **11** 67
[13] Balzarotti A 1983 *EXAFS and Near-Edge Structure Springer Series in Chemical Physics* vol 27, ed A Bianconi, L Incoccia, S Stipcich (New York: Springer) pp 130–4
[14] Brouder C, Kappler J P and Beaurepaire E 1990 *2nd European Conference on Progress on X-ray Synchrotron Radiation Research* vol 25, ed A Balerna, E Bernieri and S Mobilio (Bologna: SIF) pp 19–22
[15] Poumellec B, Cortes R, Tourillon G and Berthon J 1990 *2nd European Conference on Progress on X-ray Synchrotron Radiation Research* vol 25, ed A Balerna, E Bernieri and S Mobilio (Bologna: SIF) pp 23–6
[16] Cartier C and Verdaguer M 1989 *J. Chim. Phys.* **86** 1607
[17] Natoli C R and Benfatto M 1986 *J. Physique Coll.* **47** C8 11
[18] Foulis D L 1988 *PhD Thesis* University of Warwick
[19] Hara S 1970 *J. Phys. Soc. Japan* **22** 710
[20] Chou S H, Rehr J J, Stern E A and Davidson E R 1987 *Phys. Rev.* B **35** 264
[21] Sainctavit Ph, Petiau J, Benfatto M and Natoli C R 1989 *Physica* B **158** 347
[22] Hedin L and Lundqvist S 1969 *Solid State Phys.* **23** 1
[23] Bragg L and Claringbull G F 1965 *Crystal Structures of Minerals* (London: G Bell and Sons Ltd)
[24] Durmeyer O, Kappler J P, Beaurepaire E, Heintz J M and Drillon M 1990 *J. Phys.: Condens. Matter* **2** 6127
[25] Tossell J A, Vaughan D J and Johnson K H 1974 *Am. Mineral.* **59** 319
[26] Michel-Calendini F M, Chermette H and Pertosa P 1979 *Solid State Commun.* **31** 55
[27] Topol I A and Rambidi N G 1985 *Chem. Phys.* **92** 299
[28] Bianconi A, Garcia J, Benfatto M, Marcelli A, Natoli C R and Ruiz-López M F 1991 *Phys. Rev.* B **43** 6885
[29] Di Cicco A, Pavel N V, Bianconi A, Benfatto M and Natoli C R 1986 *J. Phys. Coll.* **47** C8 71
[30] Bugaev L A, Gegusin I I, Novakovich A A and Vendrinskii R V 1986 *J. Phys. Coll.* **47** C8 101